Supplementary Information for

Multi-synergetic ZnO Platform for High Performance Cancer Therapy

Nirmalya Tripathy,[a] Rafiq Ahmad,[b] Hyun Ah Ko,[a] Gilson Khang,[a] and Yoon-Bong Hahn[b,*]

[a] *Department of BIN Fusion Technology and Polymer BIN Research Center,* [b]*School of Semiconductor and Chemical Engineering and Nanomaterials Processing Research Center, Chonbuk National University, 567 Baekje-daero, Deokjin-gu, Jeonju 561-756, Republic of Korea.*

** Corresponding author. E-mail: ybhahn@chonbuk.ac.kr.*

Table of contents

1. Experimental Details

1.1. Synthesis of ZHS and ZNR

ZHS were prepared via two-step method. In step-I, ZnO nanospheres were synthesized by dissolving zinc nitrate hexahydrate (0.007 M) and hexamethylenetetramine (HMTA; 0.007 M) in 100 mL distilled water with the subsequent addition of sodium citrate tribasic (0.002 M). The clear solution was refluxed with cleaned Si (100) substrate at 80 °C for 1 h. Then, the ZnO nanospheres deposited substrate was removed, washed in DI water and preceded for the next step. In step-II, ZnO hollow spheres were synthesized by taking zinc nitrate hexahydrate (0.01 M), HMTA (0.01 M) and sodium citrate tribasic (0.001 M) in 100 mL DI water and the solution pH = 9 was maintained by the addition of NH_4OH. The above solution was heated at 80 °C for 1 h in a three-necked refluxing reactor with the step I resulted products. Finally, the substrate with ZHS was washed several times with DI water and dried at room temperature. ZNR as a comparative material, were synthesized by dissolving zinc nitrate hexahydrate (0.05 M) and HMTA (0.05 M) in 50 mL distilled water followed by heating in a laboratory oven for 3 h at 80 °C.

The structural morphology and crystallinity of as-synthesized ZHS and ZNR were examined by field emission scanning electron microscopy (FESEM), transmission electron microscopy (TEM), high-resolution TEM (HRTEM) equipped with the selected area electron diffraction (SAED) pattern, X-ray diffractometer (XRD) with Cu-Kα radiation (λ = 1.54178 Å) in the range of 20-70° with 8°/min scanning speed. The hydrodynamic diameter of ZHS and ZNR were measured with a dynamic light scattering (DLS) particle size analyzer (ELSZ-2, Otsuka Electronics Co., Ltd., Osaka, Japan). The optical properties were characterized by Raman scattering measurements with Ar^+ (513.4 nm) as the exciton source.

1.2. DNR encapsulation and in vitro release response

ZHS and ZNR aqueous solution (200μg/mL) were mixed with 20μg/mL DNR (daunorubicin). After adequate stirring for 12 h under dark conditions, the DNR-loaded ZnO complexes (ZHS-DNR and ZNR-DNR complexes) were centrifuged and washed with PBS until no visible red color was noticeable in the supernatant to ensure the complete removal of unbound DNR molecules. The obtained ZHS-DNR and ZNR-DNR complexes were re-suspended in PBS and stored in 4 °C for subsequent *in vitro* DNR release and cytotoxicity tests. The encapsulation of DNR molecules into the ZHS and ZNR were determined by UV-visible absorbance at 480 nm

recorded on a UV-1601 spectrophotometer. A calibration curve was plotted by taking the absorbance values of standard DNR concentration solutions and the following equation was obtained i.e. y = 0.0115x + 0.3539, where 'y' is the absorbance values and 'x' is DNR concentration (Fig. S1).[1a] From this equation, the DNR weight in supernatant of ZHS-DNR and ZNR-DNR complexes were calculated to be 2.46 and 9.4 µg, respectively. Hence, the concentration of loaded DNR into ZHS-DNR and ZNR-DNR complexes were calculated as 17.54 and 10.6 µg, respectively. Furthermore, the DNR encapsulation efficiencies were estimated using the following equations: [1b]

Drug encapsulation efficiency (%) = 100 × (Total DNR - DNR in supernatant/Total DNR)

The DNR encapsulation efficiencies for ZHS-DNR and ZNR-DNR complexes were equals to 87.7±4.10 and 53±5.76, respectively. Furthermore, DNR encapsulation was confirmed by measuring the zeta potential by a zeta potentiometer and room-temperature photoluminescence (PL) spectroscopy.

Drug release response from ZHS-DNR and ZNR-DNR complexes was also studied at endosomal/lysosomal pH 5 and physiological pH 7.4 (37 °C). In each experiment, drug-encapsulated complexes were re-suspended in PBS solutions at different pH values for various time spans (3, 6, 9, 12, 18, 24, 30 and 36 h). The release of encapsulated DNR from the complexes over time were removed from the solution by centrifugation and measured by UV-visible spectra. Additionally, in order to check the stability of the ZHS-DNR complexes, we have suspended the complexes in physiological pH = 7.4 (PBS solution) at 37 °C for 2 weeks; followed by centrifugation and measurement by UV-visible spectra.

1.3. Cell culture

Human alveolar adenocarcinoma A549 cells lines were purchased from Korean Cell Line Bank (Seoul, South Korea) and subcultures in DMEM containing L-glutamine (200 mg/L) supplemented with 10% (v/v) heat-inactivated FBS, 100U/mL penicillin and 100µg/mL streptomycin and maintained in a humidified incubator at 37 ^{o}C and 5% CO_2.

In order to minimize the aggregation propensity of ZnO structures, the particles synthesis, drug encapsulation and their solution concentrations were prepared prior to the *in vitro* studies. Additionally, before each experiment, the solutions should be sonicated to obtain mono-dispersed particles solutions.

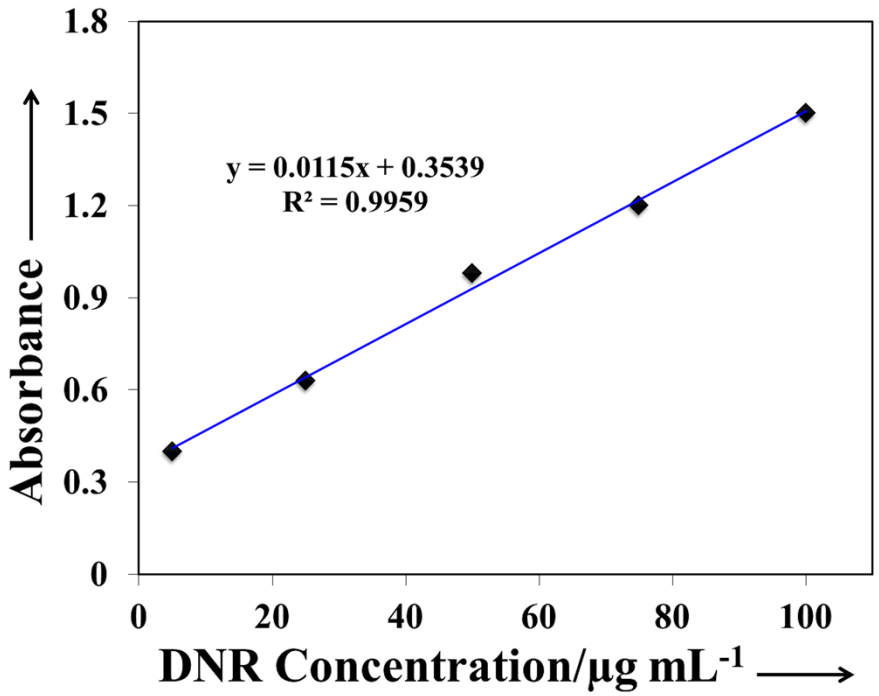

Fig. S1 Concentration-absorbance standard curve for free DNR concentration at 480 nm (optical path = 1 cm). Solid line is the liner fit obtained by the analysis tool in Origin software.

1.4. Cellular internalization and localization of DNR

The A549 cells were cultured in various concentrations of free DNR (0.25, 0.5, 1 and 2 μg/mL), ZHS-DNR and ZNR-DNR complexes (3.125, 6.25, 12.5 and 25 μg/mL) at 37 °C for 6 h. After the treatment, cells were PBS washed in order to avoid nonspecific absorbed drug, and harvested in PBS buffer at 4 °C. Then, the DNR uptake by A549 cells was measured by flow cytometer. The cellular internalization of DNR was visualized under confocal laser scanning microscopy (CLSM) at $\lambda_{excitation}$ = 488 nm, $\lambda_{emission}$ = 515 nm (LSM 510 META, Carl Zeiss). To determine the intracellular localization, cells were stained with 50nM LysoTracker Red DND-99 for 30 min to visualize lysosomes. Finally, all the captured images were processed with image analysis software (LCS image browser).

1.5. Cytotoxicity assay

The cytotoxic effects of ZHS-DNR and ZNR-DNR complexes were studied by MTT assay. Briefly, cells (10^4/well) were seeded in 96-well culture plates prior to the treatments, and incubated for 24 h at 37 °C. Next, the cells were incubated with various concentrations (3.125,

6.25, 12.5, 25, 50 and 100 µg/mL) of free DNR, ZHS, ZNR, ZHS-DNR and ZNR-DNR complexes in dark environment without any light exposure. In order to study the ZnO photodynamic anticancer effects, cells were exposed to UV irradiation (0.1mW/cm^2) for 3 min using germicidal UV lamp after 6 h incubation with the above complexes. All the cells were incubated for 48 h. After the exposure, the medium was replaced with 200 mL/well of MTT solution (0.8 mg/mL in PBS) and incubated for 4 h at 37 °C. Then, 200 mL/well of acidified isopropanol was added, kept for 4 h to solubilize the formed formazan crystals and the absorbance was measured at 570 nm using a microplate reader (DYNEX Technology, Chantilly, VA, USA).

1.6. Apoptosis study

Apoptosis induced in A549 cells was measured after treating with free DNR (1 µg/mL) and ZHS-DNR complex (12.5 µg/mL) for 24 h in the absence/presence of 3 min UV irradiation after 6 h incubation using Annexin V-FITC/PI apoptosis assay Kit according to the manufacturer's instructions. At least 10^6 cells were collected and detected by flow cytometer (FACS Canto II Analyzer) within 15 min.

1.7. Intracellular ROS assay

The intracellular ROS generation was evaluated using a commonly used ROS fluorescent probe i.e. 2'7'-dichlorofluorescein diacetate (DCFH-DA). Briefly, cells (10^5/well) were treated with ZHS and ZHS-DNR complex (12.5 µg/mL; in the absence/presence of 3 min UV irradiation) for 24 h, washed with HBSS buffer and incubated with 100 mM DCFHDA solution for 30 min at 37 ^{o}C. Finally the cell samples were lysed in alkaline solution, centrifuged and the fluorescence of supernatant was analysed using a microplate reader at 485 nm excitation and 520 nm emission.

1.8. Statistical analysis

All data were expressed as means ± Standard Deviation (SD) of experiments performed in triplicate. Statistical significance was analysed using one-way analysis of variance (ANOVA) followed by Dunnett's multiple comparison test (with the assistance of Graph pad software). *P values <0.05 is accepted to indicate statistical significant differences.

2. Characterization

2.1. Characterization of ZnO nanospheres (Step-I): TEM image (a) and XRD pattern (b) of ZnO-$Zn(OH)_2$ microspheres grown in step-I are shown in Fig. S2. TEM image (a) displays the spherically shaped ZnO-$Zn(OH)_2$ nanospheres having solid and smooth outer surfaces with diameter of ~600 nm. The XRD pattern (b) shows that the step I resulted products are composites of wurtzite $Zn(OH)_2$ and ZnO.[2]

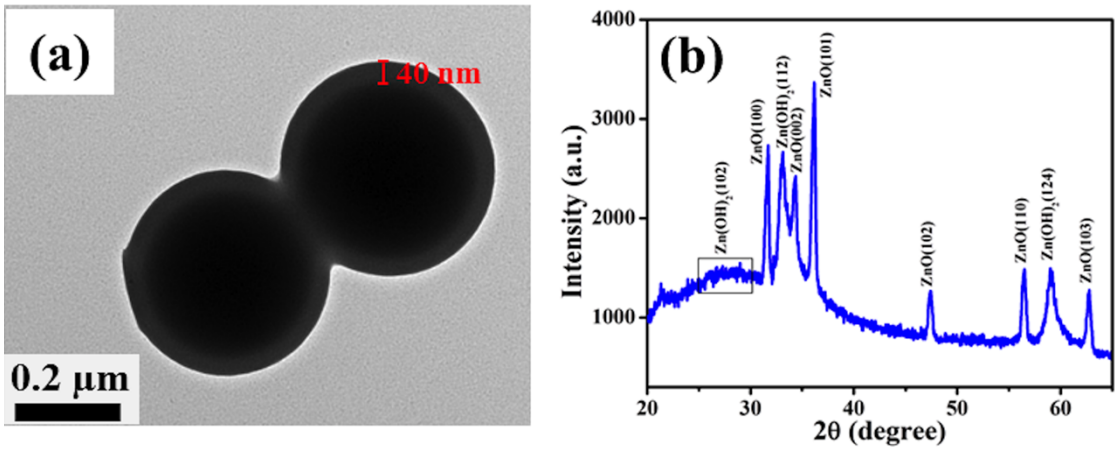

Fig. S2 (a) Low-magnification TEM image and (b) XRD pattern of the ZnO-$Zn(OH)_2$ nanospheres formed in step-I.

2.2. Crystal phase and optical property of ZnO hollow spheres: Fig. S3 shows the crystallinity and optical properties of ZHS analyzed by XRD (a) and Raman spectroscopy (b). All peaks in the XRD pattern belong to hexagonal wurtzite phase (JCPDS Card no. 36-1451). The clear and prominent peak at 439 cm^{-1} in Raman spectra is attributed to Raman-active optical-phonon E_2 mode for wurtzite ZnO.[3] Notably, no significant peak at 586 cm^{-1} was noticed attributed to the E_1 (LO) mode due to the crystal structural defects and impurities such as oxygen vacancies, zinc interstitials, etc. Hence, the appearance of high intensity, sharp and dominated E_2 mode with the absence of E_1 (LO) peak in the Raman spectra substantiates that ZHS grown are good in crystal quality with hexagonal wurtzite crystal structure. Additionally, the zeta potential value at pH 7.4 for ZHS is calculated as -21.43.

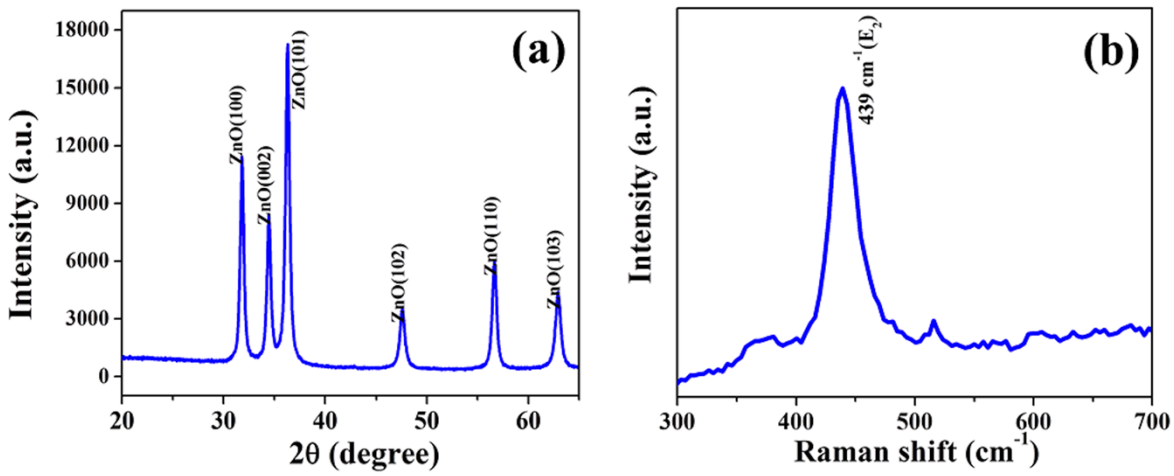

Fig. S3 (a) XRD pattern and (b) and room temperature Raman spectra of as-synthesized ZHS formed in step II.

2.3. Crystal phase and optical property of ZnO nanorods: All the observed peaks in the XRD pattern are well-matched with the reported values of wurtzite hexagonal phase pure bulk ZnO (JCPDS Card No. 75-1526), shown in Fig. S4a. A strongest peak at 34.2° attributed as ZnO (0002) in the pattern confirming that the ZNR are grown along the [0001] direction in preference, which is well-matched with HRTEM and SAED analysis. Fig. S4b shows the Raman scattering of the ZnO NRs. The appearance of a dominated, strong and sharp peak at 437 cm^{-1}, attributed to the Raman active optical phonon E_2 mode for the wurtzite hexagonal phase of ZnO. Two weak peaks at 332and 379 cm^{-1} are also observed, which are assigned to be as E_{2H}-E_{2L} (multi phonon process) and A_{1T} modes, respectively. No peaks for E_{1L} mode are observed in the spectra which demonstrate good quality. Additionally, the zeta potential value at pH 7.4 for ZNR is found as -10 mV.

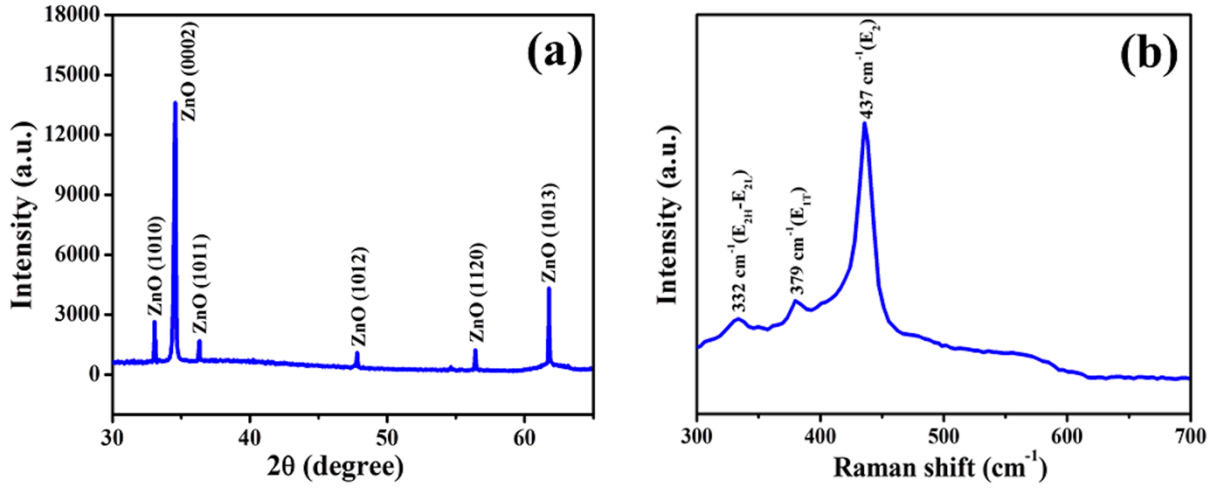

Fig. S4 (a) XRD pattern and (b) room temperature Raman spectra of ZNR.

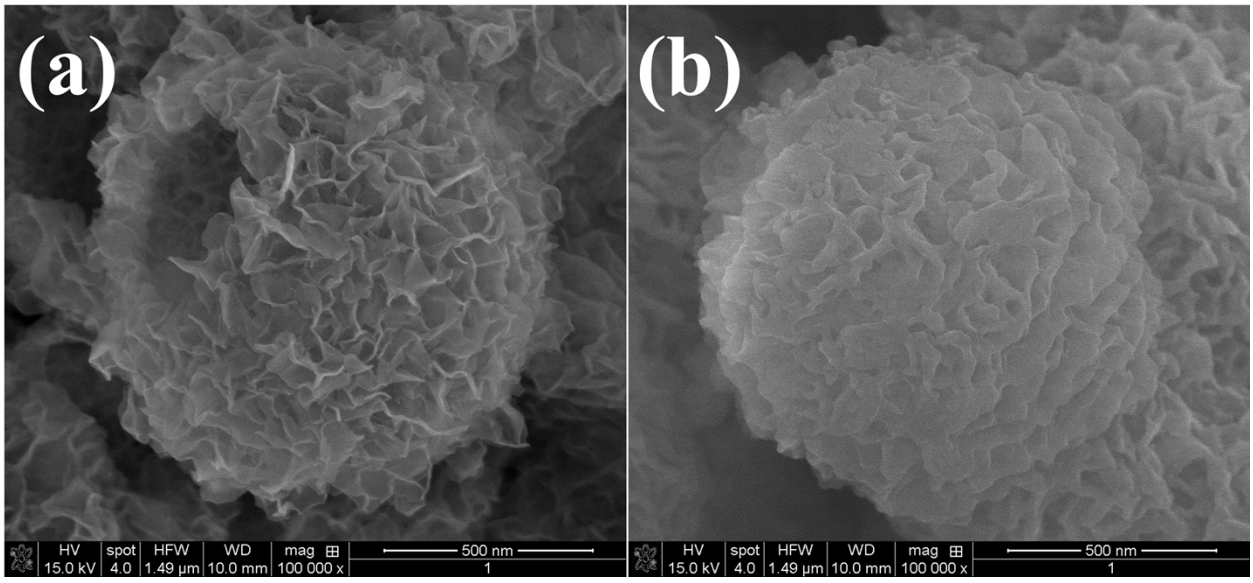

Fig. S5 FESEM images of (a) ZHS only and (b) drug loaded ZHS.

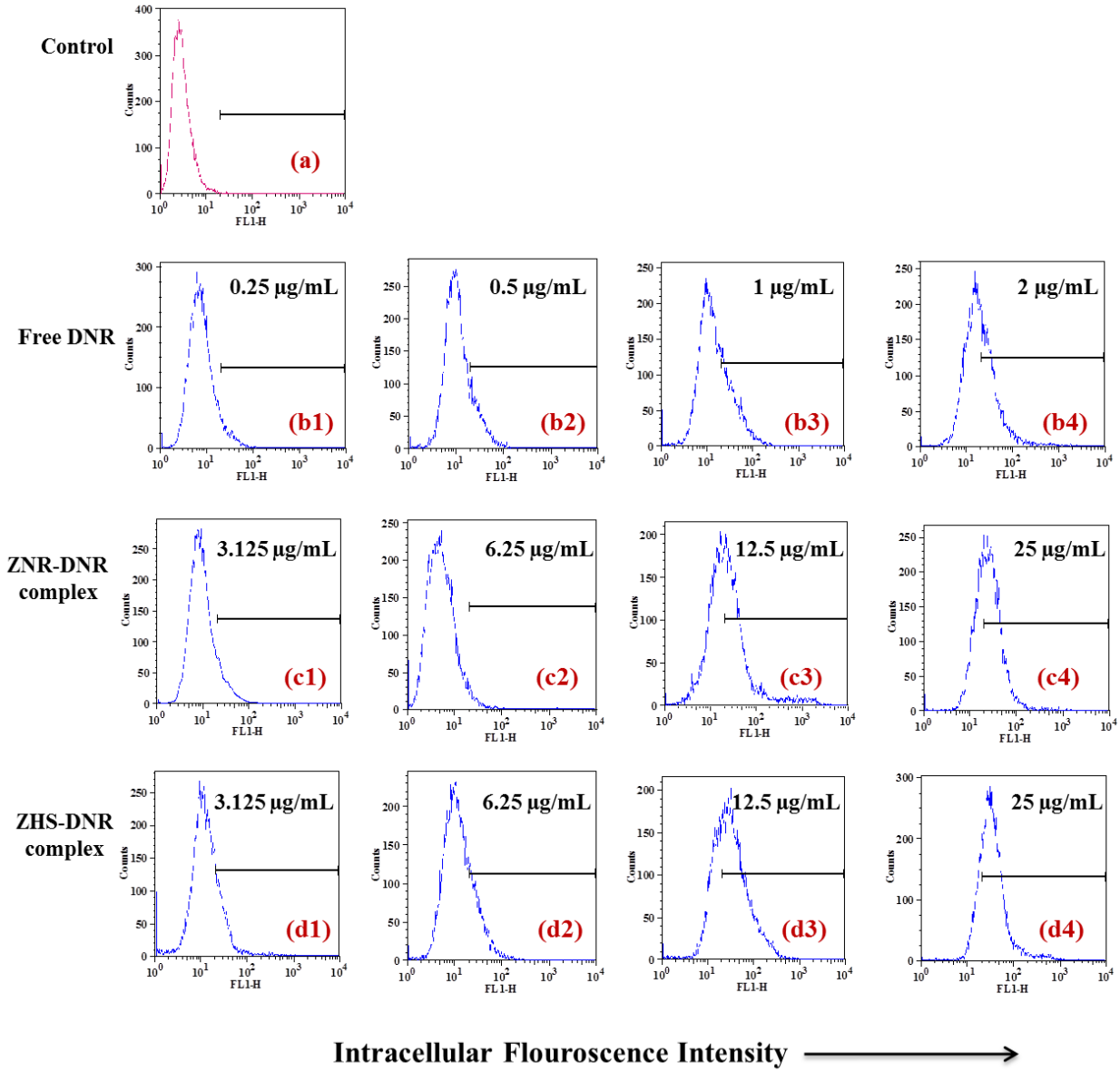

Fig. S6 Flow cytometric analysis of the total intracellular fluorescence intensity in A549 cells after 6 h exposure to free DNR (b1-b4), ZNR-DNR (c1-c4) and ZHS-DNR (d1-d4) complexes at different concentrations. (c1) 3.125μg/mL ZNR-DNR with 0.165μg/mL DNR; (c2) 6.25μg/mL ZNR-DNR with 0.33μg/mL DNR; (c3) 12.5μg/mL ZNR-DNR with 0.66μg/mL DNR; (c4) 25μg/mL ZNR-DNR with 1.3μg/mL DNR. (d1) 3.125μg/mL ZHS-DNR with 0.27μg/mL DNR; (d2) 6.25μg/mL ZHS-DNR with 0.54μg/mL DNR; (d3) 12.5μg/mL ZHS-DNR with 1.09μg/mL DNR; (d4) 25μg/mL ZHS-DNR with 2.19μg/mL DNR.

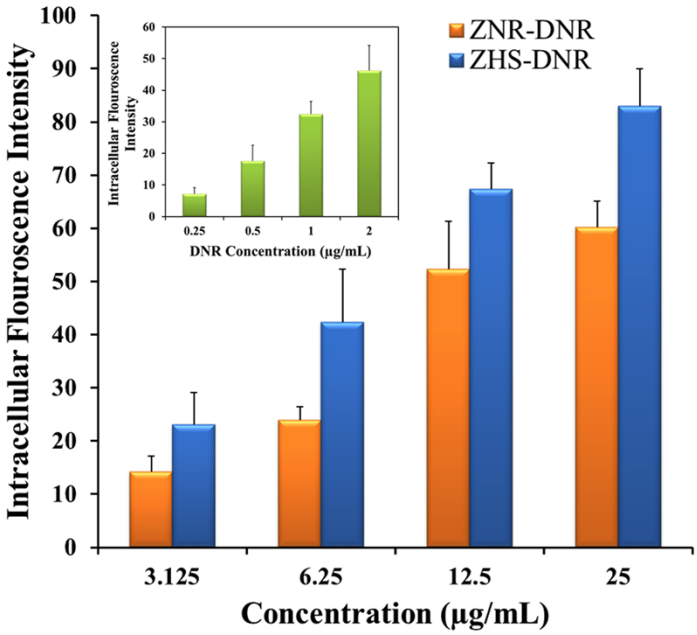

Fig. S7 Histogram representation of the intracellular fluorescence intensity in A549 cells after 6 h exposure to free DNR, ZNR-DNR and ZHS-DNR complexes at different concentrations. Each treatment was performed three times independently.

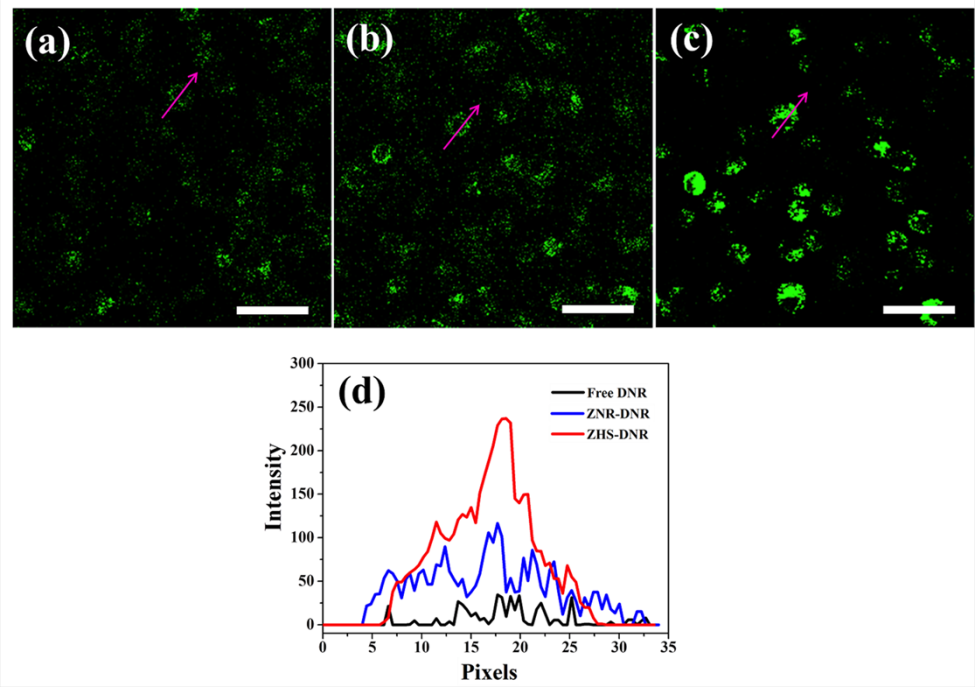

Fig. S8 CLSM images of A549 cells treated with (a) free DNR (b) ZNR-DNR and (c) ZHS-DNR complexes for 6 h. (d) The fluorescence intensity curves correspond to the CLSM images, as indicated. The scale bar is 50μm.

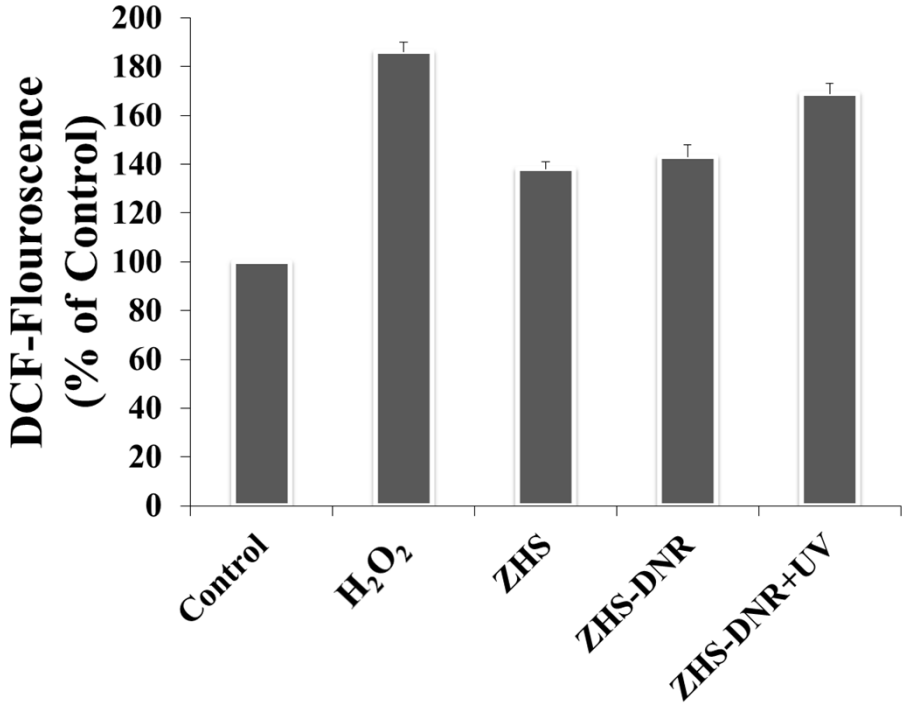

Fig. S9 Intracellular ROS and oxidative assault profiling. Cells incubated with ZHS and ZHS-DNR complex (12.5 µg/mL; in the absence/presence of 3 min UV irradiation) for 24 h. Cells without any treatment and H_2O_2 treated serves as negative and positive control, respectively. Each treatment was performed three times independently. * $p < 0.05$ *vs* control cells.

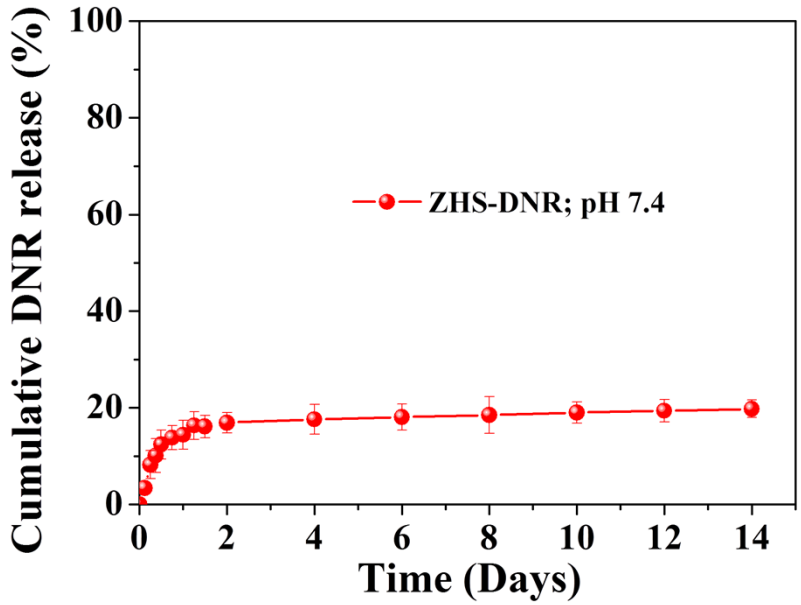

Fig. S10 Cumulative DNR release percentage from the ZHS-DNR complexes at 37 °C in physiological pH = 7.4.

In order to check the stability of the ZHS-DNR complexes, we have suspended the complexes in physiological pH = 7.4 (PBS solution) at 37 °C for 2 weeks (Figure S10). The release of encapsulated DNR from the complex were removed from the solution by centrifugation and measured by UV-visible spectra. We observed that the approximately 19% DNR was released after 14 days of storage in physiological pH = 7.4, thus suggesting considerable retention in the body.

Reference

1. (a) F. Peng, Y. Su, X. Wei, Y. Lu, Y. Zhou, Y. Zhong, S.-T. Lee and Y. He, *Angew. Chem. Int. Ed.*, **2013**, *52*, 1457; (b) F. Zhao, G. Shen, C. Chen, R. Xing, Q. Zou, G. Ma and X. Yan, *Chem. Eur. J.*, **2014**, *20*, 6880.

2. X. Wu, K. Li, H. Wang, *J. Hazard. Mater.*, **2010**, *174*, 573.

3. L. Li, H. Yang, G. Qi, J. Ma, X. Xie, H. Zhao, F. Gao, *Chem. Phys. Lett.,* **2008**, *455*, 93.